Mechanical Spectroscopy of Side-Chain Liquid Crystalline Polymers in the Glass Transition Range

S. Etienne*

Laboratoire de Métallurgie Physique et Science des Matériaux, URA CNRS 155, Ecole des Mines de Nancy, Parc de Saurupt, 54042 Nancy Cedex, France

L. David

Groupe d'Etude de Métallurgie Physique et Physique des Matériaux, URA CNRS 341, Institut National des Sciences Appliquées, 69621 Villeurbanne Cedex, France

M. Mitov and P. Sixou

Laboratoire de Physique de la Matière Condensée, URA CNRS 190, Université de Nice—Sophia Antipolis, 06108 Nice Cedex 2, France

K. L. Ngai

Naval Research Laboratory, Washington, D.C. 20375-5320

Received March 3, 1995; Revised Manuscript Received June 7, 1995®

ABSTRACT: We report the first low-frequency mechanical relaxation measurement of molecular motions at temperatures near glass transition in side-chain liquid crystalline polymers (SCLCP) with a short alkyl spacer length of 3 in the cholesteric state. The dynamics of molecular motions involved in the liquid–glass transition of side-chain liquid crystalline polymers in the cholesteric state has been studied. The effect of thermal history or physical aging has been investigated. The measured relaxation time when plotted against normalized reciprocal temperature in the metastable equilibrium state shows that the molecular motion exhibits a "fragile" or in other words a "highly cooperative" character. The interpretation of experimental results through two compatible theoretical models suggests that the molecular motions involved in the glass transition are highly correlated in these SCLCPs. Comparison with the data of a similar SCLCP that has a long alkyl spacer length highlights the change in segmental dynamics with alkyl spacer length. In addition, the sensitivity of mechanical spectroscopy makes it possible to measure the variation of the glass transition temperature as a function of the chiral group amount.

Introduction

The dynamics of molecular degrees of freedom responsible for the liquid–glass transition of polymers, or more generally in glass-forming materials, have many interesting phenomenologies and properties which have not been fully understood. The question of how to describe the dynamics is the central issue involved in current intensive research efforts from theoretical and experimental points of view.[1,2] The problem is very difficult to solve because glass-forming materials are densely packed interacting many-body systems, which make them difficult for their dynamics to be described theoretically. Thus the liquid–glass transition has remained as a challenging and unsolved problem.

In the case of liquid crystals and liquid crystalline polymers (LCP), cooperative molecular motions responsible for the dynamical behavior and the liquid–glass transition in these materials can be even more complex. The liquid crystalline order is expected to affect significantly the dynamics of the system. For example, in a columnar chiral discotic liquid crystal, both the dynamics and thermodynamics of the glass transition in such an ordered system are highly anisotropic. The nature of the glass transition has raised many interesting questions.[3] It is expected that the study of glass transition in liquid crystalline materials will enhance our understanding of the phenomenon itself.

Side-chain liquid crystalline polymers (SCLCP) have been the subject of research in recent years.[4–12] The attention paid to SCLCP having mesogenic groups in the side chains is due to the fact that mesomorphic properties inherent in liquid crystals and the mechanical performance offered by polymeric materials are combined. Thin films can be realized with mesogens aligned by special process such as poling, surface treatments, shearing, or annealing. Potential applications of the easily orientable SCLCPs such as liquid crystal polysiloxanes include optical data storage,[13] optical notch filters,[14] the decorative sector,[15] or display and recording devices.[16–18] Most SCLCP have an alkyl spacer with various lengths separating the mesogen from the polymer backbone. The alkyl spacer $-(CH_2)_l-$ with length l is introduced to decouple the motion of the mesogen from that of the polymer. However, when the spacer length l is short, the coupling between the motions of mesogenic side groups and the main chains has to be considered. The effect of such a coupling on the glass transition when the spacer length becomes short should be a subject of interest from both the fundamental and application points of view.

In the present work, we study the glass transition of side-chain liquid crystalline polysiloxane copolymers that have a short spacer length of $l = 3$ by low-frequency mechanical spectroscopy. All previous experimental measurements on molecular motions in SCLCP have used either dielctric relaxation spectroscopy[4–12] or nuclear magnetic resonance techniques.[19,20] To the best of our knowledge, the present work is the first mechanical relaxation measurement of the molecular dynamics of SCLCP in the vicinity of the glass transition temperature T_g. Rheological measurements at temperatures

* Author to whom correspondence should be addressed.
® Abstract published in *Advance ACS Abstracts,* July 15, 1995.

0024-9297/95/2228-5758$09.00/0

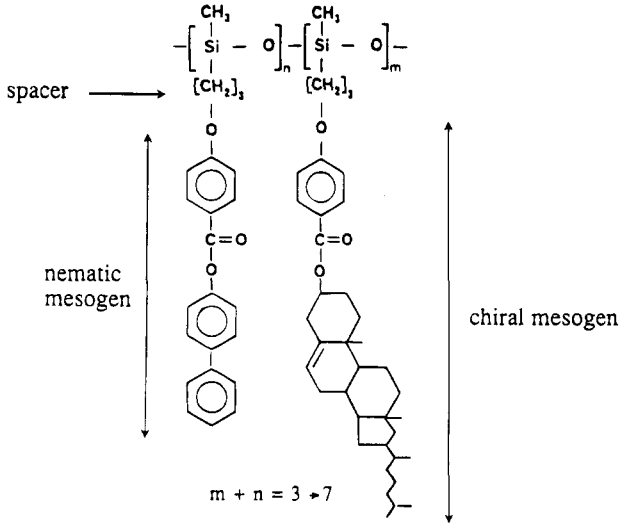

Figure 1. Chemical structure of the cholesteric side-chain liquid crystal polysiloxane.

far above T_g have been made.[21,22] The advantage of mechanical relaxation spectroscopy[23] is that the segmental motion of the nonpolar polymer main chain can be directly measured instead of indirect inference from the dielectric response of polar moieties residing in the side chain. The aim of this work is to study the dynamical behavior and the kinetic aspects of our SCLCP with short spacer length and demonstrate that the relaxation process responsible for the glass transition displays classical features such as sensitivity to thermal history and departure from the Arrhenian law. As a step further, we compare the measured normalized temperature dependency of the relaxation time in a "fragility"[24] or "cooperativity"[25,26] plot with that of another side-chain liquid crystalline polysiloxane with longer alkyl spacer length, and with those of other glass-forming materials. Interpretation of the results is made based on two compatible theoretical models.[27-29]

Experimental Section

1. Materials. The polysiloxane copolymers with a cholesterol unit in the side chain studied here were synthetized by F. H. Kreuzer according to a procedure reported elsewhere.[30-32] Polymeric materials offer an unique advantage over low molar mass compounds by the fact that the required cholesteric mesophase may be attained by annealing at an elevated temperature and locking this phase into the glassy matrix by athermal quenching. Mesogenic groups in the side chains are attached to the cyclic chain via spacers, each having three methylenes (Figure 1). Two types of mesogenic groups, a biphenyl group (nematic mesogen) and a cholesteryl group (chiral mesogen), are used. The selective Bragg reflection wavelength, and therefore the helicoidal pitch amplitude, depends on the mole fraction m/n of the chiral component. The number of siloxane units on the cyclic chain varies between 3 and 7 with 5 being the predominant case. When the m/n ratio increases, the pitch amplitude decreases, thus inducing a shift of the selective reflection wavelength from red to blue. The reflection wavelength at normal incidence can be continuously adjusted from 450 to 700 nm by mixing the four basic materials. These compounds exhibit glass transition temperatures between 40 and 55 °C, according to composition, *i.e.*, the m/n ratio, and are cholesteric up to 180–200 °C where the transition to the isotropic state occurs.

2. Mechanical Spectroscopy. Recent development in low-frequency mechanical spectroscopy has made it a very sensitive method for the investigation of molecular motions in many forms of condensed matter.[23] Experiments are carried out in the time or frequency domain. When the frequency domain is considered, results are obtained in terms of the dynamic modulus $G^*(j\omega)$:

$$G^*(j\omega) = \sigma^*(j\omega)/\epsilon^*(j\omega) = G'(\omega) + jG''(\omega) = G(\omega)\exp[j\varphi(\omega)]$$

where σ and ϵ are the stress and the strain, respectively, $\varphi(\omega)$ is referred to as the loss angle, and ω is the angular frequency. The high-resolution mechanical spectrometer used and described elsewhere[23] makes it possible to measure the complex modulus in the temperature range 77–500 K and frequency range $f = \omega/2\pi$, $1-10^{-4}$ Hz. Scanning over a wide frequency range under isothermal conditions is particularly useful for the study of the broad relaxation response due to cooperative molecular motions. The experimental setup works in torsion, and the relative strain magnitude does not exceed 10^{-5}.

The SCLCP under investigation are brittle at room temperature. Thus, in order to handle the material properly, the specimens were deposited as films (thickness about 20 μm) on low-rigidity substrates of semicrystalline PEEK previously heat treated at 170 °C (thickness about 125 μm). This material was chosen as the substrate because it presents no relaxation peak and has low loss in the temperature range involved in this study.[33] Thus, high sensitivity in the measurements of the LCPs film relaxation properties was maintained. The quantity actually measured is the complex rigidity of the composite platelet $K_m^*(j\omega)$, which can be written as

$$K_m^*(j\omega) = f_s G^*_s(j\omega) + f_{LCP} G^*_{LCP}(j\omega)$$

where f_s and f_{LCP} respectively are the shape factors and G_s^* and G_{LCP}^* respectively are the complex dynamic shear moduli of the substrate and the SCLCP film. The shape factors f_s and f_{LCP} are nearly proportional to the cube of the thickness of the substrate and the film, respectively.

This expression simplifies in the present case of a low loss substrate:

$$K_m^*(j\omega) = f_{LCP}[[f_s f_{LCP}^{-1} G'_s(\omega) + G'_{LCP}(\omega)] + jG''_{LCP}(\omega)]$$

Consequently, the measurement yields the complex modulus of the LCP film, because $G'_s(\omega)$ remains nearly constant during the experiment[33] in comparison with $G'_{LCP}(\omega)$.

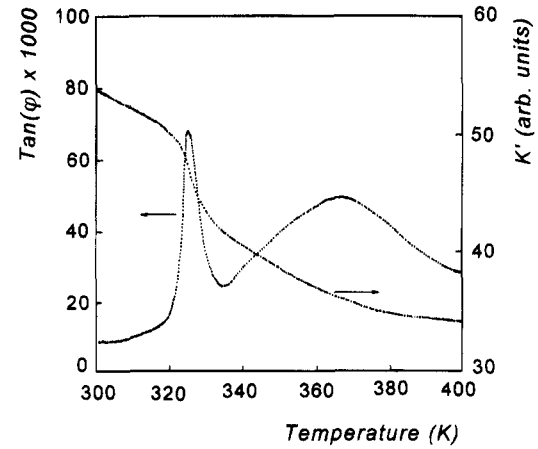

Figure 2. Isochronal tan φ and K' spectrum (at 1 Hz). The low-temperature peak corresponds to the relaxation process associated with the liquid–glass transition.

Results

First, the isochronal shear dynamic modulus was measured in the temperature range 100–450 K with a temperature scanning rate of 1 K/min. Figure 2 displays the isochronal spectrum (frequency 1 Hz) exhibited by a sample of type 1 (selective reflection in the blue region of the visible spectrum). The materials with other compositions m/n exhibited qualitatively similar

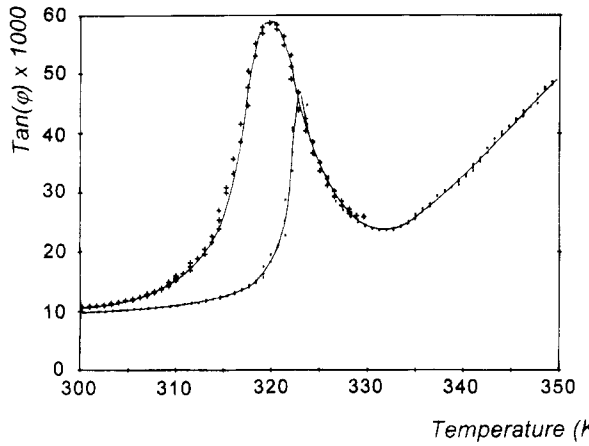

Figure 3. Isochronal spectra (1 Hz) measured on heating showing the effect of reversible physical aging at room temperature and rejuvenation on quenching: (●) after aging at room temperature; (+) second run after fast cooling from 350 K.

behavior. Two relaxation processes are observed near 325 and 350 K, respectively. Other relaxations develop at low temperatures leading to weak relaxation peaks, and these will not be considered here. The Arrhenius plot yields the characteristics of these relaxation phenomena. The low-temperature peak exhibits an apparent activation energy of 500 kJ/mol and an apparent preexponential frequency factor of about 10^{40} s^{-1}. These apparent values have orders of magnitude of the size usually encountered for the main relaxation in the liquid–glass transition range T_g of glass-forming systems. The apparent activation energy and the preexponential factor of the high-temperature peak are much lower (170 kJ/mol and about 10^{22} s^{-1}, respectively).

Figure 3 shows the effect of aging at room temperature (i.e., below the glass transition). The isochronal loss tangents, tan φ, at $f = 1$ Hz were obtained as a function of increasing temperature at a constant rate of $dT/dt = 1$ K/min. The data for a sample that had been aged at room temperature for about 10^6 s is shown in Figure 3 as the first run. After the first run, the sample was quenched from the high temperature attained to room temperature, and tan φ was measured immediately following that in the second run. It is clear on comparing the results of the two runs that the loss tangent is depressed and the peak position shifted to a higher temperature by aging. Curves resulting from first and second runs merge above 323 K. This effect was reversible, thus suggesting that crystallization did not occur during the experiments. The reversible physical aging with properties as described, and the observed departure from Arrhenius behavior, are usual features of a glass transition.

The dynamic behavior in the liquid–glass transition range was further investigated in detail by isothermal frequency scanning (1 Hz to 10^{-4} Hz) in the temperature range 298–330 K. The specimen is of type 2 (selective reflection yellow). In order to control the thermal history, each isothermal scan was carried out at decreasing temperature and after waiting 10^5 s for the system to stabilize. From these isothermal measurements, a master plot of K' and tan φ extending over 10 decades can be constructed. Figure 4 shows such a plot drawn at the reference temperature 320 K. Figure 5 is a Cole–Cole plot, K'' vs K', of the isothermal data. Strong departure from a simple Debye relaxation process is evident from the half-width of the master plot

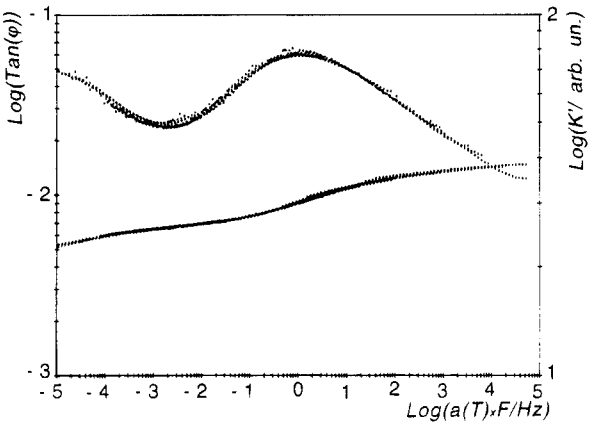

Figure 4. Isothermal complex dynamic modulus represented as a master plot. The reference temperature is 324 K. The low-frequency part of the plot below 10^{-3} Hz corresponds to the high-temperature peak of Figure 2.

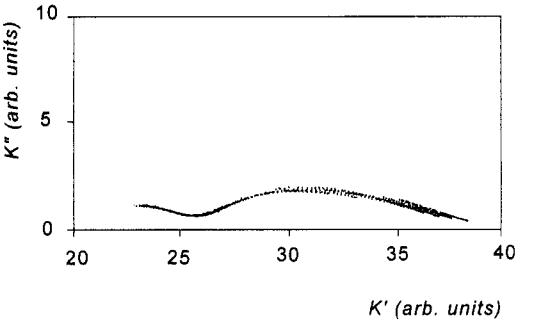

Figure 5. Isothermal complex dynamic modulus plotted as a Cole–Cole diagram. The left part of the diagram is due to the high-temperature relaxation process.

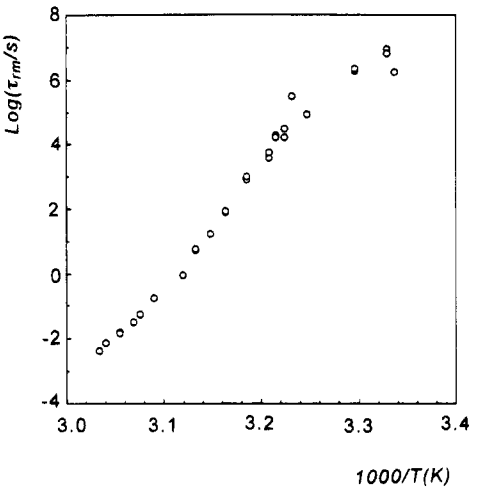

Figure 6. Variation of the molecular relaxation time (log scale) as a function of the reciprocal temperature.

and the distorted shape of the Cole–Cole plot from a semicircle.[34] A characteristic molecular relaxation time τ_{mol} is obtained as a function of temperature from $\tau_{mol} = 1/\omega_{max}$, where ω_{max} is the angular frequency at which isothermal $G''_{LCP}(\omega)$ is maximum. At temperatures where the plot of $G''_{LCP}(\omega)$ data has no maximum in the frequency window, the relaxation time was assessed by the shift factor used to construct the master curve, which assumes time and temperature equivalence. The temperature dependence of τ_{mol} is shown in Figure 6. Notwithstanding the scatter of experimental data, two regimes can be distinguished. The high-temperature regime ($T > 310$ K) corresponds to a condition of

equilibrium state and the temperature dependence resembles that of Vogel–Fulcher or the WLF equation. Below 310 K, an Arrhenius temperature dependence is observed with a rather high apparent activation energy of about 270 kJ/mol. The temperature 310 K can be regarded as the glass transition temperature corresponding to a structural relaxation time of 10^5 s, i.e., to a very slow cooling rate. The low-temperature regime below 310 K corresponds to a frozen-in isostructural state. Part of the data in Figure 6, *i.e.*, those at temperatures above 310 K, were taken under equilibrium conditions.

Different glass-forming liquids in general have different glass temperatures. However, the temperature variations of their equilibrium relaxation dynamics can be objectively compared if we plot the logarithm of a dynamic quantity such as the viscosity η or the relaxation time of the mode responsible forthe glass transition against the normalized reciprocal temperature, T^*/T. The reference temperature T^* is close to the glass temperature T_g assessed under the usual conditions and is operationally defined as the temperature at which the dynamic quantity attains an arbitrarily chosen large value like $\eta(T_g) = 10^{12}$ Pa s if viscosity is chosen[24] or $\tau(T_g) = 10^2$ s if relaxation time is chosen.[25,26] Note that shear viscosity is not a good choice if polymer is involved because the viscosity of a polymer explicitly depends on chain length. It has been repeatedly demonstrated[24–26,35,36] that meaningful comparison between the relaxation dynamics of different glass-forming liquids can be obtained from such a plot. A steeper decrease of log τ with decreasing T_g/T is often used as an indication that the glass former is more "fragile",[24] although a more appropriate connection is to increase dynamical constraints between the relaxing species (*i.e.*, increase in degree of cooperativity of the relaxation process).[25,26,35] It is interesting to plot in a similar way that part of the data of our SCLCP shown in Figure 6 that is taken under equilibrium conditions and compare its normalized temperature dependence with that of other glass formers.[24–26,35] The comparison will be made using the product $G_\infty\tau_{mol}$, where G_∞ is the glassy modulus obtained as the high-frequency limit of the measured shear modulus of our SCLCP. The temperature dependence of the product coming primarily from τ_{mol} is shown in Figure 7. This product can now be compared with similar quantities for other polymers including poly(ether sulfone)[33,36] and polyisobutylene[25,26] and with the shear viscosity of nonpolymeric glass formers such as the van der Waals liquid, *o*-terphenyl, and inorganic networks, SiO_2 and $3Na_2O{\cdot}SiO_2$. The comparison in Figure 7 shows that our SCLCP has a very steep normalized temperature dependence, indicating that it is a very "fragile"[24] or a highly cooperative relaxation[25,26,35,36] system. Previously it was established phenomenologically from experimental data of many other glass-forming liquids that steep normalized temperature dependence is usually observed together with a high sensitivity to physical aging. This correlation holds also for our SCLCP as can be seen from the experimental data given by Figures 3 and 7.

Taking into consideration the long duration of the experiment, the possiblity of a crystallization process must be considered. However, the occurrence of crystallization can be ruled out in view of the reversible aging at room temperature observed after the complete experimental run, in agrement with the results of Figure 3. We took advantage of the sensitivity of the mechanical spectroscopy method to determine the variation of the glass transition temperature T_g as a function of cholesteric group concentration. This temperature T_g, usually measured by means of DSC, is close to the temperature of the maximum of the imaginary component of the complex modulus when the measurement frequency is about 1 Hz. Experimentally we found T_g increases with the chiral group from 322 to 327 K in the concentration domain investigated.

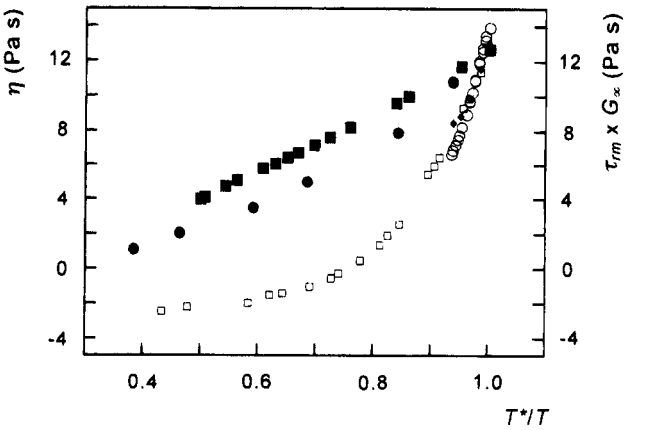

Figure 7. Representation of the variation of the molecular relaxation time in a reduced diagram, showing the fragile character of the side-chain LCP in comparison with more classical glass-forming liquids. T^* is the reference temperature where the viscosity is 10^{12} Pa s: (■) SiO_2; (●) $SiO_2{\cdot}3Na_2O$; (□) *o*-terphenyl; (◆) poly(ether sulfone); (○) SCLCP. The product of τ_{rm} (nearly equal to τ_{mol}) with the modulus at infinite frequency is used instead of the zero shear viscosity for both polymers because we are interested in the segmental motion responsible for the glass transition.

Discussion and Conclusion

To extract information on the molecular dynamics of the liquid–glass transition from the dependences of the dynamic modulus on temperature and frequency, some theoretical approach is needed. The case under consideration is complex, due to the coupling between translational and rotational degrees of freedom. In addition, for our SCLCP the liquid–glass transition is believed to involve the motion of siloxane segments coupled, via the short spacers $(CH_2)_3$, to the motion of mesogenic groups. We are interested only in the lower temperature α relaxation process (see Figures 4 and 5) in our SCLCP, which has the complicated dynamics as discussed. The higher temperature relaxation process, which we shall not further discuss, was attributed to 180° rotations of the mesogenic side groups around the main chains.[11] In the literature there are two models of relaxation in densely packed intermolecularly coupled systems that bear a strong similarity. One is the model based on nanofluctuations of density and hierarchical constraints.[27,28] The other is the coupling model.[29] Some results and interpretations of the two models are nearly the same, even though the theoretical bases of the two models differ. The present data of SCLCP offer an excellent opportunity to use both models to discuss the same set of experimental data.

1. Fluctuations and Hierarchical Constraints-Based Model (FHC Model). Despite the complexity of the bilayer structure[37] and of the mechanism suggested to be involved in the liquid–glass transition of this system, a simple modeling of dynamical behavior of disordered matter[27,28] is considered to assess the basic

aspect of molecular motions. This modeling is based on the concepts of (i) spatiotemporal fluctuations of cohesion which is shown to be present at a nanoscopic scale[38] and (ii) correlation effects among molecular motions. The key quantity yielded by this description is the molecular relaxation time τ_{mol} resulting from slowing-down dynamics and expressed as a function of microscopic physical parameters:

$$\tau_{mol} = t_0(\tau_1/t_0)^{1/(1-\nu)}$$

where $0 < \nu < 1$ is the correlation factor, τ_1 is the characteristic time of a primary elemental molecular motion, and t_0 is a scaling parameter. If ν approaches unity, then the correlation effects are maximum, while these effects are minimum when ν is equal to zero. In this last situation, the molecular motions proceed independently and the dynamic of the system is described by a molecular relaxation time equal to τ_1. This expression is similar to that proposed by the coupling model,[29] but there is an important difference. The elemental event in the FHC model is identified to be that which gives rise to the secondary relaxation and the correlation factor is linked to the microstructure, *i.e.*, disorder or fluctuation amplitude (ν decreases when the disorder increases). Within the frame of this model, the fragility of glass-forming systems is connected to the variation of the correlation parameter on temperature, *i.e.*, structure, above T_g which is consistent with the strong physical aging effect as reported on Figure 3.

Theoretical development leads to the expression of the time-dependent compliance (time domain) or the dynamic modulus $G^*(j\omega)$ (frequency domain) with the pertinent parameter τ_{mol}.

The value of the factor ν is extracted from the Cole–Cole diagram in the high frequency limit according to

$$\lim_{\omega\to\infty}\left(\frac{\partial G''}{\partial G'}\right) = -\tan\left[(1-\nu)\frac{\pi}{2}\right]$$

The value obtained from the plot of Figure 5 is $\nu = 0.76$. This large value means that a high level of correlation exists among molecular motions involved in the relaxation process linked to the liquid–glass transition, in agreement with the mechanism proposed above. The value of the activation enthalpy of the elemental event ΔH_1 can be deduced by combination of the apparent activation energy E_{app} below T_g and the value of the correlation parameter according to

$$\Delta H_1 = E_{app}(1-\nu)$$

With $\nu = 0.76$ and $E_{app} = 270$ kJ/mol, we find $\Delta H_1 = 68$ kJ/mol.

This value of ΔH_1 is compatible with the secondary relaxation process encountered in most polymeric systems.

We turn now to the fragility of the liquid state and its implication at the microscopic level. The comparative plots in Figure 7 show clearly that the siloxane LCP considered in this study exhibits a very fragile behavior. This fragile behavior is consistent with the high value of the correlation parameter ν, as previously reported.[36]

2. Coupling Model. Many previous applications of the coupling model to polymer viscoelasticity and particularly to segmental relaxation[25,26,29,35,39] have shown that it is relevant for the description of motions in densely packed systems. The description of the coupling model can be found in these earlier works. We mention briefly its theoretical basis and recent developments for the purpose of showing the similarity as well as difference with the FHC model. Molecules in a polymer interact with each other via van der Waals forces that are well described by the Lennard-Jones potential. As a general consequence of classical Newtonian or Hamiltonian mechanics, the nonlinear interaction potential will cause the motion in phase space to be *chaotic*.[40] Consideration of an irreversible process in chaotic Hamiltonian systems[41–43] leads to the existence of a microscopic time scale, t_c. At short times before t_c, chaos in phase space has not yet been developed and consequently the nonlinear interaction has no effect on the dynamics of relaxation, which proceeds with time approximately as $\exp[-(t/\tau_0)]$. After t_c, nonlinear interactions cause self-similar structure in phase space to develop, the relaxation rate is slowed to have the form $\tau_0^{-1}(\omega_c t)^{-n}$ and the correlation function has the Kohlrausch stretched exponential form $\exp[-(t/\tau^*)^{1-n}]$. Here n is the coupling parameter lying within the range, $0 \le n < 1$, and it increases with the dynamic constraints that impede independent motion of the relaxing units. The crossover of $\exp[-(t/\tau_0)]$ to $\exp[-(t/\tau^*)^{1-n}]$ at a microscopic time t_c, the essence of the coupling model, has been observed in quasielastic neutron scattering experiments.[44] The continuity requirement, $\exp[-(t_c/\tau_0)] = \exp[-(t_c/\tau^*)^{1-n}]$, of the correlation function at $t = t_c$ gives a relation between τ^* and τ_0:

$$\tau^* = t_c[\tau_0/t_c]^{1/(1-n)}$$

which is similar to the equation for τ_{mol} derived from the FHC model when the quantities of the coupling model τ^*, t_c, τ_0, and n are identified respectively with τ_{mol}, t_0, τ_1, and ν. Hence, most of the interpretations given above by the other model remain valid in the coupling model.

Along the line of recent work of relating monomer chemical structure to characteristics of segmental motion using the coupling model[25,26,29,35,39] let us discuss once more the steep normalized temperature dependence of τ_{mol} or τ^* observed in our side-chain liquid crystal polysiloxane that has an alkyl spacer with length equal to 3 (see Figure 7). Since the spacer length is not long we can expect the coupling between the motions of the siloxane segment and the mesogenic groups to be appreciable. Had it been possible to make the material with zero spacer length, one can imagine the coupling between them would be so strong that the bulky mesogenic group moves in concert with the backbone and contributes significantly to the intermolecular dynamic constraints impeding segmental motion. This extreme case should have a large coupling parameter n. When the alkyl spacer is introduced and as its length becomes longer, the motion of the polymer backbone is increasingly decoupled from that of the mesogenic group, as originally proposed by Finkelman and co-workers.[4] Not only a more decoupled polysiloxane backbone motion without involving the mesogen will see less dynamic constraints but also the increasing presence of the flexible alkyl chains in its environment will reduce the coupling parameter n. If the alkyl chain is sufficiently long, fluctuations of the concentration of methylene molecules near the siloxane backbone become inevitable and contribute to additional inhomogeneous broadening of the segmental relaxation spectrum beyond that given by the Kohlrausch stretched exponen-

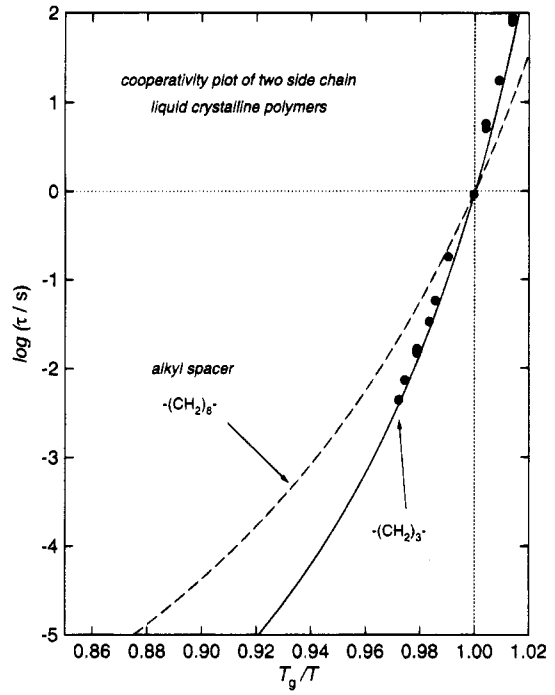

Figure 8. Comparison of the steepness of the normalized temperature dependences of the relaxation time of our SCLCP with that of another similar polysiloxane SCLCP with an alkyl spacer length of 8.

tial $\exp[-(t/\tau^*)^{1-n}]$. This is possibly the reason why the dielectrically measured α relaxation spectra of SCLCP with long alkyl spacer lengths are very broad.[5-12] Hence the coupling parameter n (and also the parameter ν in the FHC model) can no longer be determined from the width or shape of the relaxation spectrum of a SCLCP with long alkyl spacer length. Thus, even though we expect the coupling parameter of a SCLCP with long spacer length to be smaller than that of another having short spacer length, this expectation cannot be verified by comparing their segmental relaxation spectrum. However, all is not lost because, according to the coupling model,[25,26,29,39] the steepness of the normalized temperature dependence is proportional to the coupling parameter. We are led to expect that the normalized temperature dependence of our SCLCP with a short spacer length of 3 will be significantly steeper than that of another similar SCLCP with longer spacer length. In Figure 8 we plot $\log(\tau_{mol})$ against T_g/T where $\tau_{mol}(T)$ are the mechanical relaxation times of our SCLCP shown previously in Figure 6 and T_g is now defined as the temperature at which $\tau_{mol}(T_g) = 1$ s. The reason for this choice of the definition of T_g is because we shall consider dielectric data taken on side-chain liquid crystalline polysiloxanes, which are usually taken in a higher frequency range that has a lower limit in the neighborhood of about 1 Hz. In fact, we have plotted in Figure 8 the dielectric relaxation times τ_d obtained from the peak frequencies f_{max} of isothermal dielectric loss data by the formula $\tau_d = 1/(2\pi f_{max})$ of a similar side-chain liquid crystalline polysiloxane polymer having an alkyl spacer length of 8. The normalization temperature T_g of the dielectric data is defined similarly by $\tau_d(T_g) = 1$ s. By inspection of Figure 8 it is clear that indeed the normalized temperature dependence of our SCLCP with short spacer length is steeper than that of the other SCLCP with long spacer length, as we expected from the coupling model consideration.

Our future work on SCLCP will be the investigation of the properties of cross-linked systems which combine the properties of elastomers and the study in more detail of the effect of the spacer length.

References and Notes

(1) International Conferences on Relaxation in Complex Systems: Heraklion, 1990. Proceedings published in: *J. Non-Cryst. Solids* **1991**, *131–133*, 1–1266. Alicante, 1993. Proceedings published in: *J. Non Cryst. Solids* **1994**, *170–172*, 1–1440.
(2) International Workshop on Dynamics of Disordered Materials II, Grenoble, 1993. Proceedings published in: *Physica A* **1993**, *201*, 1–452.
(3) Möller, M.; Wendorf, J. H.; Werth, M.; Spiess, H. W. *J. Non-Cryst. Solids* **1994**, *170*, 295.
(4) Finkelman, H.; Rehage, G., *Adv. Polym. Sci.* **1984**, *60/61*, 99–172. Finkelman, H.; Happ, M.; Portugall, M.; Ringsdorf, H. H. *Makromol.Chem.* **1978**, *179*, 254.
(5) Shibaev, V. P.; Platé, N. A. *Adv. Polym. Sci.* **1984**, *60/61*, 173–252.
(6) Kresse, H.; Shibaev, V. P. *Makromol. Chem., Rapid Commun.* **1984**, *5*, 63.
(7) Zentel, R.; Strobl, G. R.; Ringsdorf, H. *Macromolecules* **1985**, *18*, 960.
(8) Akari, K; Attard, G. S.; Kozak, K.; Williams, G.; Gray,G. W.; Lacey, D.; Nestor, G. *J. Chem. Soc. Faraday Trans.* **1988**, *84*, 1067.
(9) Attard, G. S.; Williams, G. *Liq. Cryst.* **1986**, *1*, 253. Attard, G. S.; Akari, K.; Moura-Ramos, J. J.; Williams G. *Liq. Cryst.*, **1988**, *3*, 861.
(10) Vallerien, S. U.; Kremer, F.; Boeffel, C. *Liq. Cryst.*, **1989**, *4*, 79.
(11) Faubert, F.; Gilli, J. M.; Sixou, P.; Dandurand, J.; Lacabanne, C. *Mol. Cryst. Liq. Cryst.* **1990**, *178*, 133.
(12) Zhong, Z. Z.; Schuele, D. E.; Smith, S. W.; Gordon, W. L. *Macromolecules* **1993**, *26*, 6403. Zhong, Z. Z.; Schuele, D. E.; Gordon, W. L. *Liq. Cryst.* **1994**, *17*, 199.
(13) Pinsl, J.; Brauchle, C.; Kreuzer, F. H. *J. Mol. Electron.* **1987**, *3*, 9.
(14) Tsai, M. L.; Chen, S. H.; Jacobs, S. D. *Appl. Phys. Lett.* **1989**, *54*, 24.
(15) Eberle, H. J.; Miller, A.; Kreuzer, F. H. *Liq. Cryst.* **1989**, *5*, 907.
(16) Simon, R.; Coles, H. J. *Polymer* **1986**, *27*, 811.
(17) Simon, R.; Coles, H. J. *Liq. Cryst.* **1986**, *1*, 281.
(18) Nakamura, T.; Ueno, T.; Tani, C. *Mol. Cryst. Liq. Cryst.* **1989**, *169*, 167.
(19) Pschorn, U.; Spiess, H. W.; Hisgen, B.; Ringsdorf, H. *Makromol. Chem.* **1986**, *187*, 2711.
(20) Oulyadi, H.; Lauprêtre, F.; Sergot, P.; Monnerie, L.; Mauzac, M.; Richard, H. *Macromolecules* **1991**, *24*, 2800.
(21) Fabre, P.; Veyssie, M. *Mol. Cryst. Liq. Cryst. Lett.* **1987**, *4*, 99.
(22) Kannan, R. M.; Kornfield, J. A.; Schwenk, N.; Boeffeld, C. *Macromolecules*,**1993**, *26*, 2050.
(23) Etienne, S. In *Mechanical Spectroscopy in Materials Science*; Magalas, L., Ed.; Elsevier: Amterdam, in press.
(24) Angell, C. A. In *Relaxations in Complex Systems;* Ngai, K. L., Wright, G. B., Eds.; U.S. Government Printing Office: Washington, DC, 1994; p 3. Angell, C. A. *J. Non-Cryst. Solids* **1991**, *131–133*, 13.
(25) Plazek, D. J.; Ngai, K. L. *Macromolecules* **1991**, *24*, 1222.
(26) Böhmer, R.; Ngai, K. L.; Angell. C. A.; Plazek, D. J. *J. Chem. Phys.* **1993**, *99*, 4201.
(27) Perez, J.; Cavaillé, J. Y.; Etienne, S.; Jourdan, C. *Rev. Phys. Appl.* **1988**, *23*, 125.
(28) Etienne, S. *J. Phys. C2* **1992**, *2*, 41.
(29) For the earliest works, see for example: Ngai, K. L. *Comments Solid State Phys.* **1979**, *9*, 127, 141. For a recent review, see: Ngai, K. L. In *Disorder Effects on Relaxational Processes*; Richert, R., Blumen, A., Eds.; Springer-Verlag: New York, 1994; pp 89–150.
(30) Kreuzer, F. H. *Freiburger Arbeistagung Flussigkristalle* **1981**, 5 (Proceedings 11).
(31) Kreuzer, F. H.; Gawhary, M.; Winkler, R; Finkelmann, H. E.P. 0060335, 1981.
(32) Kreuzer, F. H.; Andrejewski, D.; Haas, W.; Haberle, N.; Riepl, G.; Spes, P. *Mol. Cryst. Liq. Cryst.* **1991**, *199*, 345.
(33) David, L.; Etienne, S. *Macromolecules* **1993**, *26*, 4489.
(34) The measurement with a composite sample as done here does not affect the shape of the Cole–Cole diagram although it causes a shift on the real axis.

(35) Ngai, K. L.; Roland, C. M. *Macromolecules* **1993**, *26*, 6824.
(36) David, L.; Sekkat, A.; Etienne, S. *J. Non-Cryst. Solids* **1994**, *172–174*, 214.
(37) Bunning, T. J.; Klei, H. E.; Samulski, E. T.; Crane, R. L.; Linville, R. J. *Liq. Cryst.* **1991**, *10*, 445.
(38) Achibat, T.; Boukenter, A.; Duval, E.; Mermet, A.; Aboulfaraj, M.; Etienne, S.; G'Sell, C. *Polymer* **1995**, *36*, 251.
(39) For recent examples, see: Plazek, D. J.; Zheng, X. D.; Ngai,K. L. *Macromolecules* **1992**, *25*, 4920. Ngai, K. L.; Plazek, D. J.; Bero, C.; *Macromolecules* **1993**, *26*, 1065. Ngai, K. L.; Roland, C. M. *Macromolecules* **1994**, *27*, 2454. Roland, C. M.; Santangelo, P.; Ngai, K. L.; Meier, G. *Macromolecules* **1993**, *26*, 6164.
(40) *Hamiltonian Dynamical Systems*; MacKay, R. S., Meiss, J. D., Eds.; Adam Hilger: Bristol and Philadelphia, 1987.
(41) Ngai, K. L.; Peng, S. L.; Tsang, K. Y. *Physica A* **1992**, *191*, 523.
(42) Ngai, K. L.; Roland; Greaves, G. N. *J. Non-Cryst. Solids*, in press.
(43) Ngai, K. L.; Tsang, K. Y. *Macromolecular Chemistry and Physics; Macromol. Symp.*, in press.
(44) Colmenero, J.; Arbe, A.; Alegria, A. *Phys. Rev. Lett.* **1993**, *71*, 2603.

MA9502922